



1 **Hydro-stochastic interpolation coupling with Budyko approach for spatial**
2 **prediction of mean annual runoff**

3 Ning Qiu^{a,b}, Xi Chen^{a,b*}, Qi Hu^c, Jintao Liu^{a,b}, Richao Huang^{a,b}, Man Gao^{a,b}

4

5 ^a *State Key Laboratory of Hydrology-Water Resources and Hydraulic Engineering*
6 *Hohai University, Nanjing 210098, China*

7 ^b *College of Hydrology and Water Resources, Hohai University, Nanjing 210098, China*

8 ^c *School of Natural Resources, University of Nebraska-Lincoln, Lincoln NE 68583, U.S.*

9 *Corresponding author E-mail: xichen@hhu.edu.cn

10



11 Abstract

12 Hydro-stochastic interpolation method based on traditional block-kriging has often
13 been used to predict mean annual runoff in river basins. A caveat in this method is that
14 the statistic technique provides little physical insight on relationships of the external
15 forcing of climate and landscape and basin runoff. In this study, the spatial runoff is
16 decomposed into a deterministic trend and stochastic fluctuations around it. The former
17 is described by the Budyko method (Fu's equation) and the latter by hydro-stochastic
18 interpolation. The coupled method of stochastic interpolation and the Budyko method is
19 applied to interpolate spatial runoff in the Huaihe River basin of China, based on outlet
20 streamflow and climate data at 40 sub-basins. Results show that the coupled method
21 significantly improves spatial interpolation accuracy of mean annual runoff. The
22 prediction errors from the coupled method are much smaller than that from the respective
23 predictions by the Budyko scheme and the hydro-stochastic interpolation. The cross-
24 validation outcome of the determination efficient, R_{cv}^2 , from the coupled method is 0.93,
25 much larger than 0.81 and 0.54 from the Budyko method and the hydro-stochastic
26 interpolation, respectively. The prediction from the coupled method describes accurately
27 the runoff distribution in the Huaihe River basin. In comparison, predictions from the
28 Budyko method and from the hydro-stochastic interpolation show substantial
29 overestimate of low runoff and underestimate of high runoff. These comparison results
30 support that the coupled hydro-stochastic interpolation with the Budyko method offers
31 an effective and accurate way in spatial interpolation of mean annual runoff.

32
33 **Keywords:** coupled Budyko-Hydro-stochastic interpolation; Mean annual runoff;



34 prediction accuracy, regional runoff

35

36 **1. Introduction**

37 Runoff at the outlet of a basin is a crucial element measuring the hydrological cycle
38 in the basin. Estimating runoffs and associated distribution pattern of water resources in
39 ungauged basins has been one of the key problems in hydrology (Sivapalan et al., 2003)
40 and a thorny issue in water management and planning (Imbach, 2010; Greenwood et al.,
41 2011). Among the existing methods for such estimation and prediction of water resources
42 availability is the regional or global runoff mapping by spatial interpolation.

43 Geostatistical approaches are mostly used in spatial interpolation. It estimates the
44 value at a given location as a weighted sum of data values at surrounding locations. The
45 spatial interpolation, assuming similarity of a generalized stochastic field (Jones, 2009),
46 uses secondary information often referred to as “multivariate” (Li and Heap, 2008). The
47 variable of interest is represented as a random field of values. Spatial similarity is
48 measured by the variance between pairs of points as a function of their Euclidian distance
49 (such as in Ordinary Kriging). Kriging has been the popular linear unbiased estimator,
50 i.e. an interpolation method in which the expected bias is zero and the expected kriging
51 error is minimized (Skøien et al., 2006). Ordinary Kriging (OK) estimates the local
52 constant mean and corresponding residuals which are regarded as random. Since the
53 spatial mean could also tell the trend tendency or nonstationary variation in space,
54 Kriging methods have been further developed into various geostatistical interpolators,
55 such as Kriging with a trend by incorporating the local trend within the neighborhood
56 search window as a smoothly varying function of the coordinates. Block Kriging (BK)



57 is also suggested as an extension of OK for estimating a block value instead of a point
58 value by replacing the point-to-point covariance with the point-to-block covariance
59 (Wackernagel, 1995). Recently, the kriging with an external drift (KED) is introduced to
60 incorporate the local trend within the neighborhood search window as a linear function
61 of a smoothly varying secondary variable instead of as a function of the spatial
62 coordinates (Goovaerts, 1997; Li and Heap, 2008).

63 Since streamflow discharge observed at the outlet represents the comprehensive
64 outcome of both precipitation and land surface over a certain drainage basin, the
65 nonstationary trend from spatial heterogeneity, regarded here as a “deterministic term”
66 at locations, exists due to distinguishingly spatial variability in climate-landscape factors,
67 such as higher or lower runoff corresponding to larger or smaller rainfall over space. The
68 spatially nonstationary trend of runoff can be interpreted by hydrological regionalization
69 in terms of hydro-climate and landscape data at various basins, e.g., developing
70 empirical relationships between runoff and its controlling factors of climate, land use
71 and topography (Qiao 1982; Arnell, 1992). Those empirical relationships obtain a
72 consensus on the form of regression equation adopted. As a simple semi-empirical
73 approach, the Budyko theory that partitions precipitation into evapotranspiration (E) and
74 runoff in regional scales based on surface water and energy balance, has been frequently
75 used (Milly, 1994; Koster and Suarez, 1999; Zhang et al., 2001; Donohue et al., 2007;
76 Li et al., 2013; Greve et al., 2014). Because Budyko method describes hydro-climate
77 relationship over a large area, its use in prediction of runoff and E in any specific
78 basins/areas still comes with large errors (Potter and Zhang, 2009; Jiang et al., 2015).



79 Many efforts have been devoted to improving Budyko method in prediction of regional
80 runoff. Improvements have been made by including land use/landcover, geomorphology
81 and climate variability in deriving parameters in Budyko method (Han et al., 2011; Li et
82 al., 2013; Yang et al., 2007; Han et al., 2011).

83 Unlike interpolating a field, such as precipitation and evaporation, to find its values
84 at “points” in space (Lenton and RodriguezIturbe, 1977; Creutin and Obled, 1982; Tabios
85 and Salas, 1985; Dingman et al, 1988; Barancourt et al, 1992 and Blöschl, 2005), spatial
86 interpolation of runoff, which is an integrated spatial continuous process in basins
87 consisting of nested sub-basins, must take into account of the river network structure
88 that constraints water balance between upstream and downstream. Previous studies have
89 indicated that without adequate spatial variation information of runoff, e.g., neglecting
90 the lateral streamflow aspects or processing basin runoff behavior as “points” in space
91 (Villeneuve et al, 1979, Hisdal and Tveito, 1993), the runoff interpolation may
92 overestimate the actual runoff (Arnell, 1995). In hydro-stochastic interpolation of runoff,
93 the upstream and downstream basin area has been treated differently from neighboring
94 basins (Sauquet et al., 2000). It has been shown that the Euclidian distances used in
95 conventional stochastic methods fail to measure the spatial distance of pairs of the
96 connected (sub)-basins in most cases.

97 Given the obvious nested structure of basins, Gottschalk (1993a, b) developed a
98 hydro-stochastic approach for runoff interpolation. It takes full account of the concept
99 that runoff is an integrated course in the hierarchical structure of the river basin system.
100 Distance between a pair of basins is measured along the river network by sub-basin



101 distance instead of Euclidian distance. A drainage basin covariogram is replacing the
102 covariogram among “points” in conventional spatial interpolation. However, in this
103 concept, spatial runoff was considered as the spatial homogeneity (Sauquet, 2006) or
104 stationarity in the “deterministic term” of the regional average runoff over basins.

105 The inclusion of the deterministic term in the original geostatistical models has been
106 shown to increase interpolation accuracy of the basin variables, e.g., mean annual runoff
107 (Sauquet, 2006) and stream temperature (Laaha et al., 2013). Nevertheless, the
108 deterministic term is mostly described by an empirical formula linking the spatial
109 features, e.g. variability of mean annual runoff with elevation (Sauquet, 2006) and
110 relationship between the mean annual stream temperature and altitude of the gauge
111 (Laaha et al., 2013). The aims of this study are to incorporate the stochastic interpolation
112 method with semi-empirical approach in quantifying the deterministic trend for spatial
113 interpolation of runoff in Huaihe River, China. In this study, the spatial runoff at sub-
114 basins is separated into the deterministic trend and its residuals, which are estimated by
115 the Budyko framework and the errors between the observed runoff and the Budyko
116 estimation. The residuals or errors were used in the hydro-stochastic interpolation
117 proposed by Gottschalk (1993a, b, 2000). After that, the runoff prediction of any specific
118 sub-basins is calculated as the total of the interpolated residual and the Budyko
119 estimation. The improved method is tested in the Huaihe River basin, China. For
120 comparison, the leave-one-out cross validation approach was applied to evaluate
121 performance of the three interpolation methods: Budyko equation, hydro-stochastic
122 interpolation, and hydro-stochastics coupling with the Budyko equation.



123 2. Methodology

124 2.1 Spatial estimation of mean annual runoff by Budyko approach

125 Budyko approach explains the variability of mean annual water balance on
 126 terrestrial scale. It describes dependence of actual evapotranspiration (E) on precipitation
 127 (P) and potential evapotranspiration (E_0) (Williams et al., 2012). The original
 128 relationship ($E/P \sim E_0/P$) derived by Budyko (1974) is deterministic and nonparametric.
 129 After the Budyko curve was applied in various basins and climate conditions, it was
 130 found also dependent on local conditions, e.g., land use/cover (Donohue et al., 2007; Li
 131 et al., 2013), soil properties (Porporato et al., 2004; Donohue et al., 2012), topography
 132 (Shao et al., 2012; Xu et al., 2013), hydro-climatic variations of seasonality (Milly, 1994;
 133 Gentine et al., 2012; Berghuijs et al., 2014) and groundwater levels (Istanbulluoglu et
 134 al., 2012). Consequently, the Budyko curve has been extended to include those effects.
 135 Some of such effects were included in parametric forms (Fu, 1981; Choudhury, 1999;
 136 Yang et al., 2008; Gerrits et al., 2009; Wang and Tang, 2014). Among all revised Budyko
 137 curves, the one-parameter equation derived by Fu (Fu, 1981, Zhang et al. 2004) has been
 138 popularly used. This equation is as follows:

$$139 \quad \frac{E}{P} = 1 + \frac{E_0}{P} - \left(1 + \left(\frac{E_0}{P}\right)^\omega\right)^{\frac{1}{\omega}} \quad (1)$$

140 or

$$141 \quad R = \left(1 + \left(\frac{E_0}{P}\right)^\omega\right)^{\frac{1}{\omega}} - E_0 \quad (2)$$

142 where P , E , E_0 and R are mean annual precipitation, actual
 143 evapotranspiration, potential evapotranspiration, and runoff (unit: mm), respectively,
 144 and ω is a dimensionless model parameter within the range $(1, \infty)$. In this formula, the



larger the ω is, the less the partitioning of precipitation into runoff.

The parameter ω can be calibrated by observed runoff at gauged basins or sub-basins in the study area. With known ω , Eq. (2) can be used for prediction of ungauged basin runoff or interpolation of spatial variation of runoff by using meteorological data in the target sub basins (Parajka and Szolgay, 1998).

2.2 Hydro-stochastic interpolation method

Gottschalk (1993a) proposed the hydro-stochastic interpolation method for spatial prediction of runoff based on Kriging interpolation. The Gottschalk's interpolation method redefined a relevant distance between drainage basins to identify the river system structure and supplement water balance constraints as follows.

As a spatial integrated continuous process, the predicted runoff in the specific unit $r^*(A_0)$ in a basin can be expressed as

$$r^*(A_0) = \sum_{i=1}^n \lambda_i r(A_i) = \Lambda^T R \quad (3)$$

where A_0 is the area of the specific unit, e.g. the basin area in this study, $r^*(A_0)$ is the predicted runoff from that basin area, $r(A_i)$ is the observed runoff in a gauged basin i with an area A_i ($i = 1, \dots, n$, n is the total number of gauged basins), λ_i is the weights of a gauged basin i , and Λ is the transposed column vector of the weights and R is the column vector of runoff $r(A_i)$.

Since $r^*(A_0)$ is the estimator of the true value $r(A_0)$, the best linear unbiased estimator requires: $E[r^*(A_0) - r(A_0)] = 0$. To achieve the goal of minimizing the estimate error, the following set of equations was developed to solve for the optimal weights given that hydrologic variables satisfy the second order stationary assumption



(Ripley, 1976)

$$\begin{cases} \sum_{j=1}^n \lambda_i C(u_i, u_j) - \mu = C_0(u_i, u_0), & i = 1, 2, \dots, n \\ \sum_{i=1}^n \lambda_i = 1 \end{cases} \quad (4)$$

where $C(u_i, u_j)$ is the fitted covariance function value between each pair of gauged basins ($i=1, \dots, n$), and $C_0(u_i, u_0)$ is the fitted covariance value between the location of interest u_0 and each of the samples u_i , μ is the Lagrange multiplier. After calculating the weights, λ_i , and substituting them into Eq. (3), the runoff prediction in the region of interest is solved by the linear combination of the weights and the observed runoff.

To calculate the weights, we write Eq. (4) into a matrix form: $C\Lambda = C_0$, and the weights matrix as

$$\Lambda = C^{-1}C_0 \quad (5)$$

where

$$C = \begin{bmatrix} Cov(u_1, u_1) & Cov(u_1, u_2) & \dots & Cov(u_1, u_n) & 1 \\ Cov(u_2, u_1) & Cov(u_2, u_2) & \dots & Cov(u_2, u_n) & 1 \\ \vdots & \vdots & \ddots & \vdots & \vdots \\ Cov(u_n, u_1) & Cov(u_n, u_2) & \dots & Cov(u_n, u_n) & 1 \\ 1 & 1 & \dots & 1 & 0 \end{bmatrix} \quad (6)$$

$$C_0 = \begin{bmatrix} Cov(u_1, u_0) \\ Cov(u_2, u_0) \\ \vdots \\ Cov(u_n, u_0) \\ 1 \end{bmatrix} \quad (7)$$

$$\Lambda = \begin{bmatrix} \lambda_1 \\ \lambda_2 \\ \vdots \\ \lambda_n \\ \mu \end{bmatrix} \quad (8)$$

Eq. (4) is the main equation set of the stochastic interpolation approach. In the runoff interpolation procedure, the fundamental unit is the block instead of point, thus matrix C represents covariance function value of the pair blocks, and matrix C_0 is the



184 covariance of block and the location of interest. The covariance values are function of
 185 block, not spatial location. Eqs. (3) and (4) only present one location to be predicted. If
 186 the interpolation procedure is multiple M non-overlapping sub-basins, Eq. (5) will be the
 187 same, but the optimal weights must be solved using the following set of equations
 188 (Sauquet and Gottschalk, 2000):

$$189 \quad \Lambda = \begin{bmatrix} L_1 \\ L_2 \\ \vdots \\ L_M \\ \mu^* \end{bmatrix} \text{ and } L_i = \begin{bmatrix} \lambda_1^i \\ \lambda_2^i \\ \vdots \\ \lambda_n^i \\ \mu^i \end{bmatrix} \quad (9)$$

190 where L_i is the weights of all the sample observations with respect to the i -th sub-
 191 basin. The matrixes C and C_0 in Eqs. (6) and (7) are

$$192 \quad C = \begin{bmatrix} K & 0 & \dots & 0 & V_1 \\ 0 & K & 0 & \vdots & V_2 \\ \vdots & 0 & \ddots & 0 & \vdots \\ 0 & \dots & 0 & K & V_M \\ V_1^T & V_2^T & \dots & V_M^T & 0 \end{bmatrix} \text{ and } C_0 = \begin{bmatrix} G_1 \\ G_2 \\ \vdots \\ G_M \\ n_T q_T \end{bmatrix} \quad (10)$$

193 In Eq. (10)

$$194 \quad K = \begin{bmatrix} Cov(A_1, A_1) & Cov(A_1, A_2) & \dots & Cov(A_1, A_n) & 1 \\ Cov(A_2, A_1) & Cov(A_2, A_2) & \dots & Cov(A_2, A_n) & 1 \\ \vdots & \vdots & \ddots & \vdots & \vdots \\ Cov(A_n, A_1) & Cov(A_n, A_2) & \dots & Cov(A_n, A_n) & 1 \\ 1 & 1 & 1 & 1 & 0 \end{bmatrix} \quad (11)$$

195 and

$$196 \quad V_i = \begin{bmatrix} n_i r(A_1) \\ n_i r(A_2) \\ \vdots \\ n_i r(A_n) \\ 0 \end{bmatrix} \quad (12)$$

$$197 \quad G_i = \begin{bmatrix} Cov(A_1, \Delta A_i) \\ Cov(A_2, \Delta A_i) \\ \vdots \\ Cov(A_n, \Delta A_i) \\ \mu^i \end{bmatrix} \quad (13)$$

198 where ΔA_i is the non-overlapping area for sub-basin i ($i = 1, \dots, M$).



199 Unlike the random point interpolation, the above set of matrix equations should be
 200 constrained by water balance, i.e., the sum of the interpolated discharge for each sub-
 201 basin should equal to the observed discharge in its river outlet. This constraint equation
 202 can be expressed specifically as

$$203 \quad R_T = \sum_{i=1}^M \Delta A_i r(\Delta A_i) \quad (14)$$

204 where R_T is total streamflow observed at outlet of the basin.

205 On grid estimation of runoff (Sauquet and Gottschalk, 2000), each of the non-
 206 overlapping areas ΔA_i is further subdivided into n_i grids surrounded by an area of a .
 207 The runoff prediction of each ΔA_i is the linear combination of weights and runoff
 208 observations presented as Eq. (15). Rearrange Eq. (14) yields

$$209 \quad R_T = \sum_{i=1}^M \left(\sum_{j=1}^{n_i} n_i \lambda_j^i r(A_j) \right) = n_T r_T \quad (15)$$

210 where n_T is the number of fundamental grids; and r_T is the runoff depth in outlet of
 211 the basin.

212 To develop the theoretical covariance function C and then the matrixes C_0 and G_0 ,
 213 the fundamental step is to define the distance between a pair of sub-basins from the
 214 identified runoff hierarchical structure in the river system. The appropriate geostatistical
 215 distance between sub-basins A and B defined by Gottschalk (1993b) is expressed as the
 216 expectation of distances of all the possible sub-basin pairs:

$$217 \quad d(A, B) = \frac{1}{A_1 A_2} \int \int_{A_1 A_2} ||u_1 - u_2|| du_1 du_2 \quad (16)$$

218 where A_1 and A_2 are the areas of sub-basin A and B.

219 Based on the sub-basin distance, an empirical covariogram versus geostatistical
 220 distance can be drawn in a scatter diagram. The theoretical covariogram $Cov(A, B)$ is



221 derived in the same way as geostatistical distance

$$222 \quad \text{Cov}(A, B) = \frac{1}{A_1 A_2} \int \int_{A_1 A_2} \text{Cov}_p(|u_1 - u_2|) du_1 du_2 \quad (17)$$

223 In the above, Cov_p is the point covariance function and can be calibrated by trial-and-
 224 error fitting method. Only independent drainage basins are used to calculate the
 225 covariance function to avoid spatial correlation of the nested drainage basins.

226

227 **2.3 Hydro-stochastic interpolation scheme with Budyko approach**

228 The above stochastic interpolation procedure assumes a stationary stochastic
 229 variation of runoff among sub-basins or spatial homogeneity in runoff features (Sauquet,
 230 2006) despite consideration of the river network structure. However, nonstationary
 231 variation of runoff from spatial heterogeneity in the river system often exists due to
 232 distinguishing spatial variability in climate-landscape factors, such as regional
 233 distribution of rainfall, evapotranspiration, topography and soils, particularly in large
 234 basins. Thus, the spatial runoff can be decomposed into nonstationary deterministic and
 235 stochastic components:

$$236 \quad R(x) = R_d(x) + R_s(x). \quad (18)$$

237 In (18), $R(x)$ is runoff at location x , $R_d(x)$ is the deterministic component of the
 238 spatial trend and/or the external drift (Wackernagel, 1995) that results in nonstationary
 239 variability, $R_s(x)$ is the stochastic component regarded as a stationary variable.

240 In this study, Fu's equation (Eq. (1)) is used as an external drift function, $R_d(x)$ in
 241 (18), accounting for the deterministic variation of mean runoff in space. The residual
 242 $R_s(x)$ [the sub-basin runoff $R(x)$ minus the external drift $R_d(x)$] is used for executing



the hydro-stochastic interpolation scheme known as “residual kriging” (Sauquet, 2006).

The sum of $R_s(x)$ and $R_d(x)$, i.e., $R(x)$ predict of runoff at ungauged sub-basins.

2.4 Cross validation

The validation procedure for (18) is conducted using leave-one-out cross-validation method (Kearns, 1999) in order to examine and compare quantitatively the performances of three prediction models (Budyko approach, hydro-stochastic interpolation, and coupling). The performance of each model is evaluated by the same metrics (Laaha and Blöschl, 2006):

$$MAE = \frac{1}{n} \sum_{j=1}^n [R(x_i) - R^*(x_i)] \quad (19)$$

$$MSE = \frac{1}{n} \sum_{j=1}^n [R(x_i) - R^*(x_i)]^2 \quad (20)$$

$$RMSE = \sqrt{\frac{1}{n} \sum_{j=1}^n [R(x_i) - R^*(x_i)]^2} \quad (21)$$

where $R^*(x)$ is the prediction of spatial variable $R(x)$. *MAE* is mean absolute error, *MSE* is mean square error, *RMSE* is root-mean-square error between prediction values and observation data.

The coefficient of determination for cross-validation is

$$R_{cv}^2 = 1 - \frac{V_{cv}}{V_{NK}} \quad (22)$$

where V_{cv} is mean square error (*MSE*); and V_{NK} is the spatial variance of the runoff over all the tested sub-basins.

The prediction result can be illustrated by regression analysis of the observation vs. prediction in addition to the evaluation metrics and R_{cv}^2 .

3. Study catchment and data

Huaihe River Basin (HRB), the sixth largest basin in China, was selected for the



validation of the spatial interpolation of runoff. HRB is of particular interest because of its situation in China's transition terrain from north to south, and the transition climate from the warm temperate monsoonal climate in the east to sub-humid climate on the west (Hu, 2008). The basin has the most human population density, and is one of the major agricultural areas in China. Millions of tons of water are consumed each year to sustain the population and agriculture. Water resources per capita and per unit area is less than one-fifth of the national average. Moreover, more than 50% of the water resources is overexploited, much higher than the recommended rate for international inland rivers (30%) (Yan et al, 2011). Higher precipitation concentration, represented by large percentages of the annual precipitation in a few very rainy months, makes the region vulnerable for severe floods as well as droughts. The frequent droughts and floods increase difficulty in water resources utilization and flood prevention (Zhang et al., 2015).

The selected study area is located upstream of Bengbu Sluice in HRB with an area of 121,000 km² (Fig. 1). The river network system is derived from data packages of National Fundamental Geographic Information System issued by National Geomatics Center of China. The area in the upstream is divided into 40 sub-basins, in terms of available hydrological stations with records within the period 1961-2000 (Fig. 2). The sub-basin area varies from the smallest of 17.9 km² (at PH station) to the largest of 30630 km² (WJB station). Among the 40 sub-basins, there are 27 independent sub-basins and 13 nested sub-basins of the observation network.

Annual precipitation data from 1961-2000 are obtained from monthly mean



climatological dataset at 0.5° spatial resolution constructed by China Meteorological Administration (available at: http://data.cma.cn/data/detail/dataCode/SURF_CLI_CHN_PRE_MON_GRID_0.5/keywords/0.5.html). Pan evaporation data at 21 meteorological stations in HRB are used to interpolate spatial potential evapotranspiration via ArcGIS, and then the annual potential evapotranspiration of each sub-basin in HRB is obtained. The statistical features of mean annual precipitation, potential evapotranspiration and runoff during the period from 1961–2000 are listed in Table 1. During 1961–2000, the mean annual precipitation P varied from 638~1629 mm; mean annual temperature was $11\sim 16^\circ\text{C}$, and the mean annual potential evaporation E_0 varied between 900~1200 mm. The sub-basins in the north are relatively dry with the dryness index (E_0/P) higher than 1.3 for the sub-basins of ZM, ZQ, XY and ZK. Sub-basins in the south are wet with the dryness index (E_0/P) lower than 0.8 for the sub-basins of MS, HBT and HC. The average mean annual runoff depth R is about 400 mm, but fluctuating from a minimum of 90 mm in the northern region near the Yellow River to a maximum of 1000mm in the south mountainous areas. The temporal and spatial variation of runoff of HRB is relatively small in the south but large in the north.

4 Results

4.1 Prediction of runoff by Fu's equation

Actual evapotranspiration E (Table 1) is estimated according to long-term mean of annual water balance ($E=P-R$). On the basis of Eq. (1) and long-term mean of annual water balance components during 1961–2000 at the 40 sub-basins (Table 1), we plot the E/P vs. E_0/P in Fig. 3. In Fig. 3, we also include the water limit line of the arid edge at



which $E = P$ and the energy limit line of the wet edge at which $E = E_0$. The curve shape in Fig. 3 is determined by the parameter ω . Its value in each sub-basin is calculated directly using Eq. (1) and is listed in Table 1. The range of ω is from the smallest 1.43 at HWH to the largest 3.16 at JJJ, the average of ω is 2.32 over the 40 sub-basins.

The sub-basin averaged ω can be fitted by minimizing the mean absolute error (*MAE*) (Legates and McCabe, 1999) between the predicted and the estimated annual evapotranspiration E from the long-term water balance (Fig. 3). The fitted value of ω for the 40 sub-basins determined from this process is 2.213, very close to the average directly from the 40 individual sub-basins.

Using $\omega=2.213$ in our study basin, Fu's Eq. (2) is written

$$R = \left(1 + \left(\frac{E_0}{P} \right)^{2.213} \right)^{\frac{1}{2.213}} - E_0. \quad (23)$$

Eq. (23) and Fig. 3 clearly show the deterministic trend of runoff in space. The smaller the index $\frac{E_0}{P}$ is, the larger the runoff is over the sub-basins in HRB. In Fig. 3, the larger R in the sub-basins in the north indicates drier conditions in those sub-basins.

Using Eq. (23) and the mean annual precipitation P and potential evapotranspiration E_0 at the 40 sub-basins given in Table 1, the predicted runoff depth by Fu's equation and deviation, or prediction error, between prediction and observation are calculated. The results are also summarized in Table 1 and 2. The *MAE* of Budyko runoff prediction is 94 mm, and the *RMSE* is 112 mm. The largest absolute error is at HWH (328.03 mm) and the smallest at XX (23.77 mm) (Table 1 and 2). The largest relative error is 91 mm at XZ station, about 81.6% of the observed runoff at the site, and the smallest is 36.94 mm at XHD, 4.99% of the observed runoff.



332

333 4.2 Hydro-stochastic interpolation of runoff

334 For comparison, direct use of the observed runoff in the hydro-stochastic
 335 interpolation is executed based on the procedure detailed in Section 2.2. The covariance
 336 was firstly calculated by

$$337 \quad C(d) = E[r(x_i) \cdot r(x_i + d)] - \bar{r}^2 \quad (24)$$

338 where \bar{r} is the average of the observed runoff among the sub-basins, d is the
 339 geostatistical distance between pairs of the sub-basins.

340 In order to obtain the distance d between the sub-basin pairs, HRB is divided into
 341 grids of 40 row \times 50 column resolution. According to Eq. (16), the geostatistical
 342 distances of all the possible sub-basin pairs (820 in this study) were calculated to obtain
 343 the average distance of each pair of grid points in sub-basins A and B. According to the
 344 estimated distance for pairs of sub-basins and the observed runoff at 40 sub-basins (Table
 345 1), the empirical covariance $C(d)$ is estimated for each pair of sub-basins. From plots
 346 of the mean estimated $C(d)$ of the independent sub-basin pairs versus the
 347 corresponding distances d with an interval of 50 km, we get an empirical covariogram
 348 shown in Fig. 4. The best fit to this empirical covariogram is

$$349 \quad C(d) = 600000 \times \exp(-d/28.62). \quad (25)$$

350 The fitted exponential function in (25) is used to calculate the theoretical covariance
 351 matrix $Cov(A, B)$ in Eq. (17). Then the matrices of C , C_0 , K , V and G are
 352 subsequently generated by MATLAB programs, and the weight coefficient matrix is
 353 calculated consequently.



354 The interpolation results over 40 sub-basins are conducted, and the prediction error
355 is shown in Table 1. The *MAE* and *RMSE* are 134 mm and 176mm, respectively. The
356 largest absolute error is at HWH (448 mm) and the smallest at XHD (3 mm) (Table 2).
357 The interpolation errors are larger than those from the Budyko curve, a result indicating
358 that the observed runoff is controlled by the deterministic trend in space, which markedly
359 affects spatial interpolation accuracy.

360

361 4.3 Hydro-stochastic interpolation with Fu's equation

362 Because of the significant deterministic trend of runoff in space, the trend removal
363 can help justify assumptions of spatially-autocorrelated random error for the hydro-
364 stochastic interpolation. Following Section 2.3, we use Fu's equation (Eq. (2)) to
365 estimate the deterministic trend or the external drift function $R_d^*(x)$, and departures of
366 the trend, or the residual/errors, between the prediction and observation. The residual
367 $R_s^*(x)$ is used for hydro-stochastic interpolation. The results are given in Table 1.

368 The empirical covariogram of $R_s^*(x)$ for each pair of sub-basins versus sub-basin
369 distances is plotted in Fig. 5. The following exponential function is obtained from the
370 best fitting the empirical covariogram

$$371 \quad C(d) = 3000 \times \exp(-d/48.34). \quad (26)$$

372 From (26), matrices C , C_0 , K , V and G in Eqs. (9) ~ (13) are calculated using
373 MATLAB, and the weight coefficient matrix of runoff deviation is then calculated to
374 predict runoff deviation. Since this interpolation scheme represents the spatial runoff
375 deviation, the sum of the interpolated runoff deviation and the simulated runoff by Fu's



equation is regarded as the total interpolated runoff in sub-basins.

Prediction outcome of runoff is listed in Table 1, with the *MAE* of 47 mm and *RMSE* of 69mm over the 40 sub-basins. The largest absolute error is at HWH (236 mm) and the smallest at JJJ (1.5 mm) (Table 2).

4.4 Comparison of spatial runoff perdition by the three approaches

As listed in Table 2, our method coupling the deterministic and stochastic processes described in this study significantly reduces the prediction errors in space. *MAE* and *RMSE* from the coupled method are much smaller than those from the Budyko and the hydro-stochastic interpolation methods. The maximum error at HWH is significantly reduced as well; 236 mm from the coupled method is much smaller than 328 mm from the Budyko method and 448 mm from the hydro-stochastic interpolation. In terms of the cross-validation outcome in Table 2, the cross-validation outcome R_{cv}^2 from our coupled method is as large as 0.93, much larger than 0.81 and 0.54 from the Budyko method and the hydro-stochastic interpolation, respectively.

The correlation analysis between predicted and observed runoff depth is shown in Fig. 6. The prediction from our coupled method is highly correlated with the prediction ($R^2=0.95$) and small deviation from the 1:1 line. In contrast, correlation between the prediction and observation from the Budyko method and the hydro-stochastic interpolation is low ($R^2=0.58$ and 0.82, respectively). Particularly, they markedly overestimate low runoff and underestimate high runoff (strong departures to 1:1 line in Fig. 6). The systematic deviation of the runoff prediction by the hydro-stochastic interpolation has also been reported in the previous work by Sauquet et al. (2000), Laaha



398 and Bloschl (2006) and Yan et al. (2011).

399 Mapping spatial distribution of runoff in HRB by the three approaches of Budyko
400 equation, hydro-stochastic interpolation and our coupled method is shown in Fig. 7.
401 There are significant differences in mapped runoff distribution in HRB by the three-
402 spatial interpolation methods. Compared with our coupled method, the Budyko method
403 and hydro-stochastic interpolation markedly underestimate sub-basin runoff in the north
404 where climate is relatively dry and runoff is small. Among the predicted runoff in the
405 largest non-overlapping area above BB, the one made by our coupled method is 125mm,
406 and the ones made by the Budyko method and the hydro-stochastic interpolation are 264
407 and 179 mm, respectively.

408 **5. Discussion and conclusions**

409 Investigating the underlying patterns of hydrological variables is important in our
410 effort to obtain good knowledge of spatial variation of the hydrological variables in a
411 region of interest. Because of existence of some degree of natural organization or
412 connection of water basins (Dooge, 1986; Sivapalan, 2005), e.g., rivers that connect sub-
413 basins, and hydro-climate similarity, we can describe the hydrological variables of
414 interest in deterministic forms of functions, curves or distributions and construct
415 conceptual and mathematical models to predict hydro-climate variability (Wagener et al,
416 2007). However, the deterministic method in describing complex patterns suffers
417 inevitable loss of information (Wagener et al, 2007) because of existence of uncertainty
418 in many hydrological processes and data. Thus, hydrological variables also contain
419 information of stochastic nature, and should be treated as outcomes of both deterministic
420 and stochastic processes. Use of combined or coupled deterministic and statistical



hydrological models to predict hydrological processes has been recommended and proven to be effective in improving accuracy of various aspects of hydrology, such as hydrological forecast (Cheng et al., 2014; Ly et al., 2013) and groundwater table interpolation (Holman et al., 2009).

In this study, we use the Budyko's deterministic method to describe mean annual runoff as an integrated spatial continuous process determined by both the hydro-climate elements and the hierarchical river system networks. A deviation from the Budyko estimation is our use of the hydro-stochastic interpolation that assumes spatially-autocorrelated random error. The predicted runoff is the coupling of predictions by the Budyko method and the hydro-stochastic interpolation. The deterministic aspects of runoff described by Budyko method reflect regional trends at positions (sub-basins) and their deviations caused by stochastic processes are determined by the weights as a function of physical distance. Weights are higher for near points/basins and are smaller for distant points/basins.

We tested our coupled method in the Huaihe River basin in China. Our results show that the coupled method outperformed both the Budyko method and the stochastic interpolation by significantly increasing the spatial interpolation and prediction accuracy. The interpolation errors in terms of *MAE* and *RMSE* from our coupled method are 47 and 69mm over the 40 sub-basins, respectively, much smaller than 94 and 112 mm from the Budyko, and 134 and 176mm from the hydro-stochastic interpolation. The maximum error at HWH is significantly reduced as well. It is 236 mm from our coupled method much smaller than 328 mm from the Budyko method and 448 mm from the hydro-



443 stochastic interpolation. The cross-validation outcome of the deterministic coefficient
444 R_{cv}^2 from our coupled method is 0.93, much larger than 0.81 and 0.54 from the Budyko
445 method and the hydro-stochastic interpolation, respectively. The prediction from the
446 coupled method captures most accurately among the three methods the regional high and
447 low runoff in the HRB.

448 Because our coupled method incorporates climate conditions, e.g., precipitation and
449 evapotranspiration, it provides a useful tool to estimate climate change impacts on long-
450 term water availability in large-scale river basins and to assess potential consequences
451 of climate change in environment and water and food security.

452

453

454 **Acknowledgement**

455 The research was supported by the National Natural Science Foundation of China
456 (No. 51190091 and 41571130071).

457

458

459 **References**

- 460 Arnell, N. W.: Factors controlling the effects of climate change on river flow regimes in
461 a humid temperate environment, *Journal of hydrology*, 132(1-4), 321-342, 1992.
462 Arnell, N. W.: Grid mapping of river discharge. *J. Hydrol.*, 167, 39-56, 1995.
463 Barancourt, C., Creutin, J. D., and Rivoirard, J.: A method for delineating and estimating
464 rainfall fields, *Wat. Resour. Res.*, 28, 1133-1144, 1992.
465 Berghuijs, W. R., Woods, R. A., and Hrachowitz, M.: A precipitation shift from snow
466 towards rain leads to a decrease in streamflow, *Nature Clim. Change*, 4(7), 583–586,
467 2014.
468 Bishop, G. D., Church, M. R., Aber, J. D., Neilson, R. P., Ollinger, S. V., and Daly, C.: A
469 comparison of mapped estimates of long term runoff in the northeast United States,
470 *Journal of Hydrology*, 206: 176-190, 1998.
471 Blöschl, G.: Rainfall-runoff modelling of ungauged catchments, Article 133, in:
472 *Encyclopedia of Hydrological Sciences*, edited by: Anderson, M. G., pp. 2061–2080,



- 473 Wiley, Chichester, 2005.
- 474 Blöschl, G., Sivapalan, M., and Wagener T.: Runoff Prediction in Ungauged Basins:
475 Synthesis Across Processes, Places and Scales, Cambridge Univ. Press, Cambridge, U.
476 K, 2013.
- 477 Budyko, M. I.: Climate and Life, Academic, New York, 1974.
- 478 Cheng, Q. B., Chen, X., Xu, C. Y., Reinhardt-Imjela, C., and Schulte, A.: Improvement
479 and comparison of likelihood functions for model calibration and parameter uncertainty
480 analysis within a Markov chain Monte Carlo scheme, *Journal of hydrology*, 519, 2202-
481 2214, 2014.
- 482 Choudhury, B.: Evaluation of an empirical equation for annual evaporation using field
483 observations and results from a biophysical model, *J. Hydrol.*, 216(1–2), 99–110, 1999.
- 484 Creutin, J. D. and Obled, C.: Objective analysis and mapping techniques for rainfall
485 fields an objective comparison, *Wat. Resour. Res.*, 18, 413–431, 1982.
- 486 Degaetano, A. T. and Belcher, B. N.: Spatial interpolation of daily maximum and
487 minimum air temperature based on meteorological model analyses and independent
488 observations, *Journal of Applied Meteorology & Climatology*, 46(11), 1981–1992, 2006.
- 489 Dingman, S. L., Seely-Reynolds, D. M. and Reynolds, R. C.: Application of kriging to
490 estimating mean annual precipitation in a region of orographic influence, *Wat. Resour.*
491 *Bull.*, 24, 329–339, 1988.
- 492 Donohue, R. J., Roderick, M. L., and McVicar, T. R.: On the importance of including
493 vegetation dynamics in Budyko's hydrological model, *Hydrol. Earth Syst. Sci.*, 11(2),
494 983–995, 2007.
- 495 Donohue, R. J., Roderick, M. L., and McVicar, T. R.: Roots, storms and soil pores:
496 Incorporating key ecohydrological processes into Budyko's hydrological model, 436-
497 437, 35–50, 2012.
- 498 Dooge, J. C. I.: Looking for hydrologic laws. *Water Resources Research* 22 (9), 46S–
499 58S, (2003). Linear theory of hydrologic systems. EGU Reprint Series (Originally
500 published in 1965), Katlenburg-Lindau, Germany, 1986.
- 501 Fu, B.: On the calculation of the evaporation from land surface (in Chinese), *Sci. Atmos.*
502 *Sin.*, 1(5), 23–31, 1981.
- 503 Gentile, P., D'Odorico, P., Lintner, B. R., Sivandran, G., and Salvucci, G.:
504 Interdependence of climate, soil, and vegetation as constrained by the Budyko curve,
505 *Geophys. Res. Lett.*, 39(19), L19404, 2012.
- 506 Gerrits, A. M. J., Savenije, H. H. G., Veling, E. J. M. and Pfister, L.: Analytical derivation
507 of the Budyko curve based on rainfall characteristics and a simple evaporation model,
508 *Water Resour. Res.*, 45, W04403, 2009.
- 509 Gottschalk, L.: Correlation and covariance of runoff, *Stochast. Hydroi. Hydraul.*, 7, 85-
510 101, 1993a.
- 511 Gottschalk, L.: Interpolation of runoff applying objective methods, *Stochast. Hydroi.*
512 *Hydraul.*, 7, 269–281, 1993b.
- 513 Gottschalk, L., Krasovskaia, I., Leblois, E., and Sauquet, E.: Mapping mean and variance
514 of runoff in a river basin, *Hydrology and Earth System Sciences Discussions*, 3(2), 299-
515 333, 2006.
- 516 Goovaerts, P.: Geostatistics for natural resources evaluation, Oxford University Press on



- 517 Demand, 1997.
- 518 Greenwood, A. J. B., Benyon, R. G., and Lane, P. N. J.: A method for assessing the
- 519 hydrological impact of afforestation using regional mean annual data and empirical
- 520 rainfall–runoff curves, *Journal of Hydrology*, 411(1–2), 49–65, 2011.
- 521 Greve, P., Orlowsky, B., Mueller, B., Sheffield, J., Reichstein, M., and Seneviratne, S. I.:
- 522 Global assessment of trends in wetting and drying over land, *Nat. Geosci.*, 7(10), 716–
- 523 721, 2014.
- 524 Han, S., Hu, H., Yang, D., and Liu, Q.: Irrigation impact on annual water balance of the
- 525 oases in Tarim Basin, Northwest China, *Hydrol. Process*, 25, 167–174, 2011.
- 526 Hisdal, H., Tveito, O. E.: Generation of runoff series at ungauged locations using
- 527 empirical orthogonal functions in combination with kriging, *Stochast. Hydrol. Hydraul.*,
- 528 6, 255–269, 1993.
- 529 Hollingsworth, A., Lönnberg, P.: The verification of objective analyses: diagnostics of
- 530 analysis system performance, *Meteorology & Atmospheric Physics*, 40(1–3), 3–27, 1989.
- 531 Holman, I. P., Tascone, D., and Hess, T. M.: A comparison of stochastic and deterministic
- 532 downscaling methods for modelling potential groundwater recharge under climate
- 533 change in East Anglia, UK: implications for groundwater resource management,
- 534 *Hydrogeology Journal*, 17(7), 1629–1641, 2009.
- 535 Hu, W. W., Wang, G. X., Deng, W., and Li, S. N.: The influence of dams on eco
- 536 hydrological conditions in the Huaihe River basin, China, *Ecological Engineering*, 33(3),
- 537 233–241, 2008.
- 538 Imbach, P. L., Molina, L. G., Locatelli, B., Roupsard, O., Ciais, P., Corrales, L., and
- 539 Mahé, G.: Climatology-based regional modelling of potential vegetation and average
- 540 annual long-term runoff for Mesoamerica, *Hydrology Earth System Sciences*, 14(10),
- 541 1801–1817, 2010.
- 542 Istanbuluoglu, E., Wang, T., Wright, O. M., and Lenters, J. D.: Interpretation of
- 543 hydrologic trends from a water balance perspective: The role of groundwater storage in
- 544 the Budyko hypothesis, *Water Resour. Res.*, 48, W00H16, 2012.
- 545 Jakeman, A. J. and Hornberger, G. M.: How much complexity is warranted in a rainfall-
- 546 runoff model? *Water Resources Research*, 29(8), 2637–2649, 2010.
- 547 Jiang, C., Xiong, L., Wang, D., Liu, P., Guo, S., and Xu, C. Y.: Separating the impacts of
- 548 climate change and human activities on runoff using the Budyko-type equations with
- 549 time-varying parameters, *Journal of Hydrology*, 522, 326–338, 2015.
- 550 Jin, X., Xu, C. Y., Zhang, Q., and Chen, Y. D.: Regionalization study of a conceptual
- 551 hydrological model in Dongjiang basin, South China, *Quaternary International*, 208(1–
- 552 2), 129–137, 2009.
- 553 Jones, O. D.: A stochastic runoff model incorporating spatial variability. 18th world
- 554 IMACS CONGRESS AND MODSIM09 International congress on modelling and
- 555 simulation: interfacing modelling and simulation with mathematical and computational
- 556 sciences, 157(1), 1865–1871, 2009.
- 557 Jutman, T.: Runoff, Climate, Lakes and Rivers: National Atlas of Sweden. Stockholm:
- 558 SNA Publishing, 106–111, 1995.
- 559 Kearns, M. and Ron, D.: Algorithmic stability and sanity-check bounds for leave-one-
- 560 out cross-validation, *Neural computation*, 11(6), 1427–1453, 1999.



- 561 Koster, R. D. and Suarez M. J.: A simple framework for examining the inter annual
562 variability of land surface moisture fluxes, *J. Clim.*, 12(7), 1911–1917, 1999.
- 563 Laaha, G. and Blöschl, G.: Seasonality indices for regionalizing low flows,
564 *Hydrological Processes*, 20(18), 3851–3878, 2006.
- 565 Laaha, G., Skøien, J. O., Nobilis, F., and Blöschl, G.: Spatial prediction of stream
566 temperatures using Top-kriging with an external drift, *Environmental Modeling &*
567 *Assessment*, 18(6), 671–683, 2013.
- 568 Legates, D. R. and McCabe, G. J.: Evaluating the use of “goodness-of-fit” measures in
569 hydrologic and hydroclimatic model validation, *Water resources research*, 35(1), 233–
570 241, 1999.
- 571 Lenton, R. L. and Rodriguez-Iturbe, I.: Rainfall network system analysis: the optimal
572 estimation of total areal storm depth, *Wat. Resour. Res.*, 13, 825–836, 1977.
- 573 Li, D., Pan, M., Cong, Z., Zhang, L., and Wood, E.: Vegetation control on water and
574 energy balance within the Budyko framework, *Water Resour. Res.*, 49(2), 969–976, 2013.
- 575 Li, J. and Heap, A. D.: A review of spatial interpolation methods for environmental
576 scientists, 137–145, 2008.
- 577 Luo, W., Taylor, M. C. and Parker, S. R.: A comparison of spatial interpolation methods
578 to estimate continuous wind speed surfaces using irregularly distributed data from
579 England and Wales, *International Journal of Climatology*, 28(7), 947–959, 2008.
- 580 Ly, S., Charles, C., and Degré, A.: Different methods for spatial interpolation of rainfall
581 data for operational hydrology and hydrological modeling at watershed scale, A review,
582 *Biotechnologie, Agronomie, Société et Environnement*, 17(2), 392, 2013.
- 583 Milly, P. C. D.: Climate, soil water storage, and the average annual water balance, *Water*
584 *Resour. Res.*, 30(7), 2143–2156, 1994.
- 585 Niehoff, D., Fritsch, U., and Bronstert, A.: Land-use impacts on storm-runoff generation:
586 scenarios of land-use change and simulation of hydrological response in a meso-scale
587 catchment in SW-Germany, *Journal of Hydrology*, 267(1–2), 80–93, 2002.
- 588 Parajka, J. and Szolgay, J. Grid-based mapping of long-term mean annual potential and
589 actual evapotranspiration in Slovakia, *IAHS Publications-Series of Proceedings and*
590 *Reports-Intern Assoc Hydrological Sciences*, 248, 123–130, 1998.
- 591 Porporato, A., Daly, E., and Rodriguez-Iturbe, I.: Soil water balance and ecosystem
592 response to climate change, *Am. Nat.*, 164(5), 625–632, 2004.
- 593 Potter, N. J. and Zhang, L.: Inter annual variability of catchment water balance in
594 Australia, *Journal of Hydrology*, 369(1), 120–129, 2009.
- 595 Qiao, C. F.: Mapping runoff isocline of Hai, Luan River basin. *Hydrology*, (s1), 63–66,
596 1982.
- 597 Ripley, B. D.: The second-order analysis of stationary point processes, *Journal of*
598 *applied probability*, 13(2), 255–266, 1976.
- 599 Sauquet, E. Mapping mean annual river discharges: Geostatistical developments for
600 incorporating river network dependencies, *Journal of Hydrology* 331, 300– 314, 2006.
- 601 Sauquet, E., Gottschalk, L., and Leblois, E.: Mapping average annual runoff: a
602 hierarchical approach applying a stochastic interpolation scheme, *Hydrological Sciences*
603 *Journal*, 45(6), 799–815, 2000.
- 604 Shao, Q., Traylen, A., and Zhang, L.: Nonparametric method for estimating the effects



- 605 of climatic and catchment characteristics on mean annual evapotranspiration, *Water*
606 *Resour. Res.*, 48, W03517, 2012.
- 607 Sivapalan, M.: Pattern, processes and function: elements of a unified theory of hydrology
608 at the catchment scale. In: Anderson, M. (ed.) *Encyclopedia of hydrological sciences*,
609 London: John Wiley, pp. 193–219, 2005.
- 610 Sivapalan, M., Takeuchi, K., Franks, S. W., Gupta, V. K., Karambiri, H., Lakshmi, V., ...
611 and Oki, T.: Iahs decade on predictions in ungauged basins (pub), 2003–2012: shaping
612 an exciting future for the hydrological sciences, *Hydrological Sciences Journal*, 48(6),
613 857–880, 2003.
- 614 Skøien, J. O., Merz, R., and Blochl, G.: Top-kriging geostatistics on stream networks,
615 *Hydrology and Earth System Sciences Discussions*, 2(6), 2253–2286, 2005.
- 616 Tabios, G. Q. and Salas, J. D.: A comparative analysis of techniques for spatial
617 interpolation of precipitation, *Wat. Resour. Bull.*, 21, 365–380, 1985.
- 618 Villeneuve, J. P., Morin, G., Bobée, B., Leblanc, D., and Delhomme, J. P.: Kriging in the
619 design of streamflow sampling networks, *Wat. Resour. Res.*, 15, 1833–184, 1979.
- 620 Wackernagel, H.: *Multivariate geostatistics*, Berlin: Springer, 1995.
- 621 Wagener, T., Sivapalan, M., Troch, P., and Woods, R.: Catchment classification and
622 hydrologic similarity, *Geography compass*, 1(4), 901–931, 2007.
- 623 Wang, D. and Tang Y.: A one-parameter Budyko model for water balance captures
624 emergent behavior in darwinian hydrologic models, *Geophys. Res. Lett.*, 41, 4569–4577,
625 2014.
- 626 Williams, C. A., Reichstein, M., Buchmann, N., Baldocchi, D., Beer, C., Schwalm, C. ...
627 and Papale, D.: Climate and vegetation controls on the surface water balance: Synthesis
628 of evapotranspiration measured across a global network of flux towers, *Water Resources*
629 *Research*, 48(6), 2012.
- 630 Xu, X., Liu, W., Scanlon, B. R., Zhang, L., and Pan, M. Local and global factors
631 controlling water-energy balances within the Budyko framework, *Geophys. Res. Lett.*,
632 40, 6123–6129, 2013.
- 633 Yan, Z., Xia, J., and Gottschalk, L.: Mapping runoff based on hydro-stochastic approach
634 for the Huaihe River Basin, China, *Journal of Geographical Sciences*, 21(3), 441–457,
635 2011.
- 636 Yang, D., Sun, F., Liu, Z., Cong, Z., Ni, G., and Lei, Z. Analyzing spatial and temporal
637 variability of annual waterenergy balance in nonhumid regions of China using the
638 Budyko hypothesis, *Water Resour. Res.*, 43, W04426, 2007.
- 639 Yang, H., Yang, D. Z. Lei, and Sun, F.: New analytical derivation of the mean annual
640 water-energy balance equation, *Water Resour. Res.*, 44, W03410, 2008.
- 641 Zhang, L., Dawes, W. R. G., and Walker, R.: Response of mean annual
642 evapotranspiration to vegetation changes at catchment scale, *Water Resour. Res.*, 37(3),
643 701–708, 2001.
- 644 Zhang, L., Hickel, K., Dawes, W. R., Chiew, F. H., Western, A. W., and Briggs, P. R.: A
645 rational function approach for estimating mean annual evapotranspiration, *Water*
646 *Resources Research*, 40(2), 2004.
- 647 Zhang, R., Chen, X. Zhang, Z. and Shi, P.: Evolution of hydrological drought under the
648 regulation of two reservoirs in the headwater basin of the Huaihe River, China,



649 Stochastic environmental research and risk assessment, 29(2), 487-499, 2015.

650

651



652 **Captions of figures:**

- 653 1. Figure 1 Topography and river network of HRB above Bengbu;
 654 2. Figure 2 Sub-basins and hydrological stations of HRB above Bengbu;
 655 3. Figure 3 Plot of $E/P \sim E_0/P$ for 40 sub-basins and Budyko curve of HRB
 656 4. Figure 4 Empirical covariogram from sub-basin runoff data and fitted covariogram
 657 of HRB;
 658 5. Figure 5 Empirical covariogram from sub-basin runoff deviation and fitted
 659 covariogram of HRB
 660 6. Figure 6 Cross validation of runoff prediction vs. observation by (a) Fu's equation,
 661 (b) hydro-stochastic interpolation, and (c) coupled method. The dotted line
 662 is 1:1;
 663 7. Figure 7 Spatial distribution of mean annul runoff: (a) Budyko; (b) hydro-stochastic
 664 interpolation; (c) coupled method
 665



666 Table 1 Summary of hydro-meteorological data and predicted runoff of sub-basins in HRB

No	Stations	Basin area\km ²	P (mm)	R (mm)	E ₀ (mm)	E ₀ /P	E (mm)	ω	Fu's Equation		Hydro-stochastic interpolation		Coupling method	
									Predicted R (mm)	Error (mm)	Predicted R (mm)	Error (mm)	Predicted R (mm)	Error (mm)
1	CTG	3090	1012	366	932	0.92	646	2.41	399	32.85	371	4.90	348	17.84
2	XHD	1431	1517	740	974	0.64	776	2.41	777	36.94	737	2.70	692	47.82
3	SQ	3094	822	168	1024	1.25	653	2.83	248	79.29	285	116.77	178	10.10
4	MS	1970	1517	672	957	0.63	845	3.06	786	114.28	584	88.45	662	10.13
5	BGS	2730	877	225	1029	1.17	651	2.57	279	53.93	247	22.39	181	44.01
6	XC	4110	945	225	997	1.06	720	3.02	332	106.82	272	46.77	212	13.11
7	BT	11280	910	223	993	1.09	687	2.85	310	86.94	275	52.25	219	3.74
8	ZK	25800	678	123	1061	1.56	555	2.54	163	39.96	228	104.65	61	61.70
9	JJJ	5930	1347	513	969	0.72	834	3.16	640	127.27	520	7.49	512	1.49
10	HB	16005	1092	335	937	0.86	757	3.15	455	120.48	334	1.02	360	25.01
11	ZQ	3410	739	118	1083	1.47	621	2.83	190	71.71	219	101.07	141	23.40
12	HPT	4370	1629	764	984	0.60	865	2.92	868	103.53	755	9.22	712	51.64
13	XX	10190	987	367	1053	1.07	620	2.10	343	23.77	381	13.73	424	56.96
14	BB	121330	850	215	1024	1.20	635	2.54	264	49.48	394	179.16	125	90.46
15	WJB	30630	1003	294	957	0.95	709	2.85	384	90.29	304	9.65	287	6.90
16	LZ	390	963	345	1078	1.12	618	2.09	320	24.96	320	25.08	399	53.75
17	NLD	1500	1019	439	1101	1.08	581	1.86	351	88.30	309	129.64	401	37.56
18	ZMD	109	690	212	1093	1.58	478	1.94	163	48.65	281	68.78	235	22.53
19	BLY	737	1504	868	1126	0.75	635	1.69	695	173.27	639	229.05	794	74.23
20	HWH	292	1560	1068	1127	0.72	492	1.43	740	328.03	619	448.83	832	236.16
21	ZC	493	1512	838	1112	0.74	674	1.79	708	130.23	695	142.77	777	61.19
22	BQY	284	1268	693	1094	0.86	575	1.68	527	166.21	349	344.06	604	89.35
23	QL	178	1559	970	1090	0.70	589	1.60	756	214.17	646	324.06	840	130.17
24	HNZ	805	1480	640	1114	0.75	840	2.41	681	41.37	577	63.05	585	55.20
25	TJH	152	1305	699	1090	0.84	605	1.74	556	143.66	262	437.02	589	110.18
26	LX	77.8	1025	484	1079	1.05	540	1.75	361	123.77	241	242.88	436	48.01
27	ZLS	1880	755	253	1104	1.46	502	1.91	194	58.45	169	84.28	233	19.94
28	ZT	501	1021	437	1101	1.08	583	1.87	351	85.87	242	195.10	411	26.08
29	XGS	375	830	302	1088	1.31	528	1.91	238	63.74	243	58.60	297	5.46



30	JZ	46	1103	583	1107	1.00	520	1.63	404	178.81	200	382.51	455	127.50
31	GC	620	638	111	1055	1.65	528	2.51	145	34.18	139	28.42	103	8.08
32	ZM	2106	645	97	1039	1.61	548	2.72	150	53.48	141	43.80	105	7.58
33	YZ	814	979	235	1083	1.11	743	2.85	329	94.07	277	42.13	246	11.24
34	XZ	1120	746	111	1040	1.39	636	3.06	202	90.66	167	56.30	152	40.95
35	GZ	1030	855	342	1098	1.28	513	1.81	250	92.10	255	86.54	307	35.14
36	DPL	1770	1067	331	1066	1.00	736	2.57	393	61.62	339	8.02	342	11.39
37	XX2	256	1301	606	1092	0.84	695	2.00	552	53.68	705	99.36	552	53.82
38	PH	17.9	1248	708	1094	0.88	540	1.61	512	196.04	604	104.35	512	195.90
39	HC	2050	1255	454	1095	0.87	802	2.54	517	63.36	363	91.02	409	44.52
40	HK	2141	871	227	1077	1.24	644	2.44	264	37.28	309	82.40	186	41.22

667

668



669

670 Table 2 Interpolation and cross-validation errors between the predicted and observed

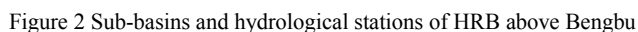
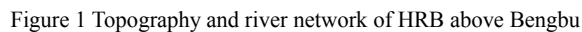
671 runoff at 40 sub-basins for the three methods

Evaluation indicators	Budyko	Hydro-stochastic interpolation	Coupling method
MAE (mm)	94	134	47
RMSE (mm)	112	176	69
Max error (mm)	328	448	236
Min error (mm)	24	3	1.5
R_{cv}^2	0.81	0.54	0.93

672

673

675
676
677



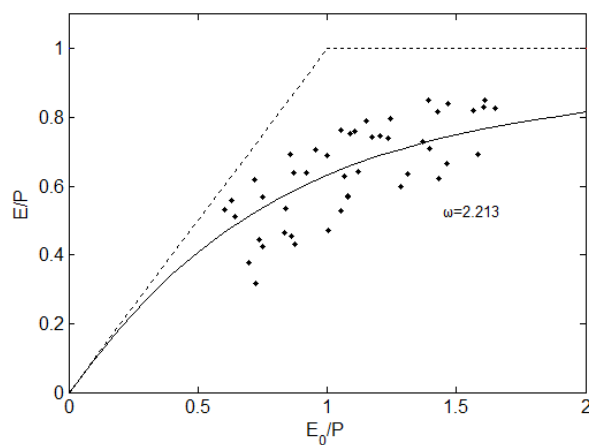
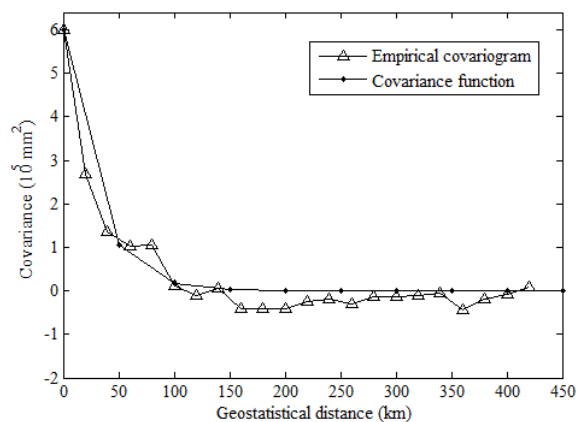


Figure 3 Plot of $E/P \sim E_0/P$ for 40 sub-basins and Budyko curve of HRB



685



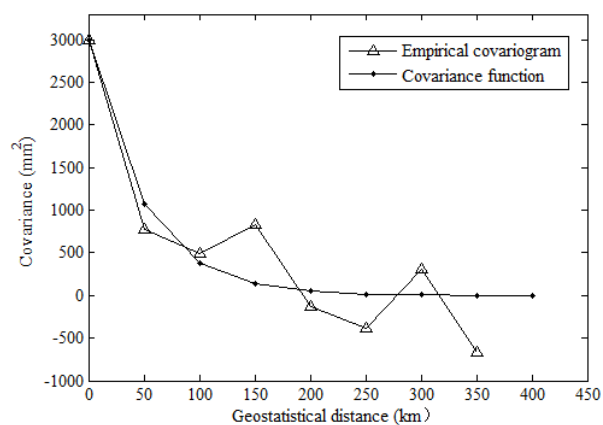
686

687

688

689

Figure 4 Empirical covariogram from sub-basin runoff data and fitted covariogram of HRB



690

691

692

693

694

Figure 5 Empirical covariogram from sub-basin runoff deviation and fitted covariogram of HRB

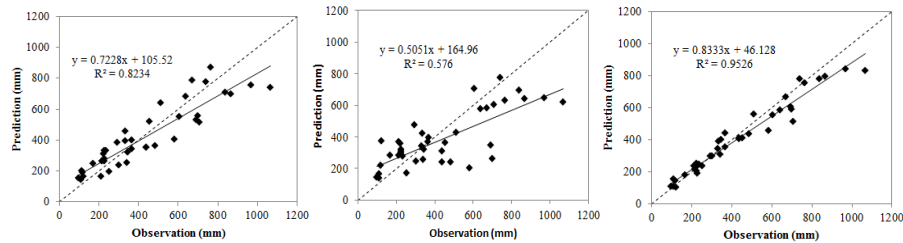


Figure 6 Cross validation of runoff prediction vs. observation by (a) Fu's equation, (b) hydro-stochastic interpolation, and (c) coupled method. The dotted line is 1:1

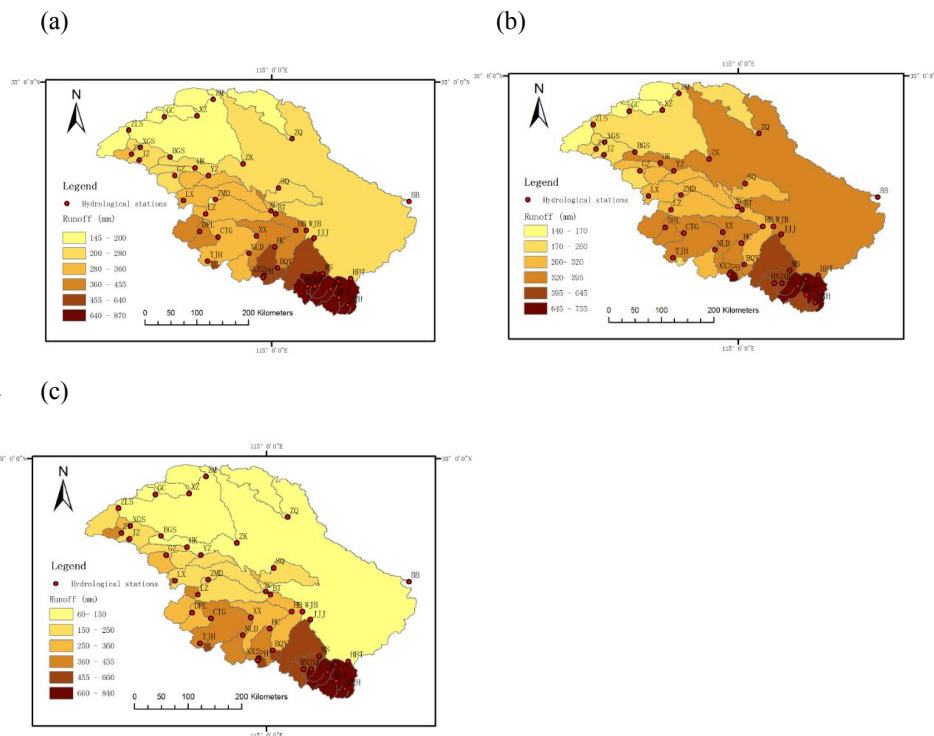


Figure 7 Spatial distribution of mean annual runoff: (a) Budyko; (b) hydro-stochastic interpolation; (c) coupled method